RADIATED SOUND AND TURBULENT MOTIONS IN A BLUNT TRAILING EDGE FLOW FIELD

Daniel W. Shannon
dshannon@nd.edu

Scott C. Morris
morris.65@nd.edu

Thomas J. Mueller
mueller.1@nd.edu

Center for Flow Physics and Control
Department of Aerospace and Mechanical Enginerring,
University of Notre Dame
Notre Dame, Indiana 46556, USA

ABSTRACT

The dipole sound produced by edge scattering of pressure fluctuations at a trailing edge is most often an undesirable effect in turbomachinery and control surface flows. The ability to model the flow mechanisms associated with the production of trailing edge acoustics is important for the quiet design of such devices. The objective of the present research was to experimentally measure flow field and acoustic variables to develop an understanding of the mechanisms that generate trailing edge noise. These measurements facilitated the study of the causal relationships between the turbulent flow field, unsteady surface pressure, and radiated farfield acoustics. Experimental methods used in this paper include Particle Image Velocimetry (PIV), unsteady surface pressure, and far field acoustic pressure. The model investigated had an asymmetric 45° beveled trailing edge. Reynolds number ranging from $1.2\text{x}10^6$ to $1.9\text{x}10^6$. It was found the small scale turbulent motions in the vicinity of the trailing edge were modulated by a large scale von Karman wake instibilities. This dependance of the broadband sound created by these motions on the "phase" of the wake instability was observed.

INTRODUCTION

Spatially correlated surface pressures are created by turbulent motions as they convect over a trailing edge. The resultant unsteady force on the model surface causes scattering of noise to the far field in the form of a dipole source. This phenomena is particularly strong in the vicinity of the a sharp trailing edge, where the geometry lends itself to generating spatially correlated surface pressure fields. The radiated acoustic energy will be dependant on the size and convection speed of the turbulent motions as they convect over the trailing edge. Previous theoretical and experimental works relating turbulent flow variables to trailing edge noise are summarized in Blake (1986) and Gershfeld and Blake (1988).

The radiated acoustic pressure can be expressed in terms of the flow field as a solution to the inhomogeneous wave equation Howe (1975):

$$\nabla^2 B + k_o^2 B = \nabla \cdot (\vec{\omega} \times \vec{u}), \qquad (1)$$

where the source term is the divergence of the vorticity-velocity cross product, k_o is the acoustic wave number, and the variable $B = p/\rho_o + u^2/2$, which consists of the far field acoustic pressure and velocity variables. In the absence of a full solution (e.g. DNS) of the velocity field, the solution to equation (1) can be estimated in a stochastic way by modeling the space-time correlation function of the velocity and vorticity, and relating these functions to radiated sound.

Experimental results are discussed in the following sections in which a unique combination of velocity, vorticity, surface pressure, and acoustic pressure have been measured on an asymmetric 45° beveled trailing edge at a Reynolds number ranging from $1.2\text{x}10^6$ to $1.9\text{x}10^6$. The airfoil was a flat strut with a 50.8mm thickness and a 0.91m chord. The leading edge was a 5:1 ellipse with boundary layer trips placed on both surfaces of the airfoil. Two unsteady surface pressure sensors were located 12.5mm upstream of the sharp trailing edge on the suction (upper) surface and pressure (lower) surface of the model. The trailing edge geometry is illustrated in Figure 1. The separation point of the upper boundary layer from the bevelled surface is noted, as are the locations of the unsteady surface pressure sensors.

Sound generated by the trailing edge can be considered to be a superposition of two types of acoustic sources: tonal and broadband. Figure 2 displays the measured sound pressure level (SPL) spectra measured at a distance of 1.08m from the center span of the sharp trailing edge in an Anechoic Wind Tunnel (AWT). The unsteady semi-periodic wake instability associated with the shedding of boundary layer vorticity into the wake is responsible for the narrowband tonal noise generated by the trailing edge. For

the model geometry under investigation the nondimentionalized shedding frequency occurs at

$$\frac{\omega y_f}{U_\infty} \sim 1 , \tag{2}$$

where ω is circular frequency, U_∞ is the free stream velocity, and y_f (~25 mm) is a wake thickness parameter determined by the minimum distance between the upper and lower shear layers (Blake, 1986). The the spectra at the tonal frequency are typically orders of magnitude greater than the broadband noise. Smaller scale turbulent motions in the vicinity of the trailing edge causes acoustic scattering at frequencies proportional to their relative size and convection velocities. This phenomena is responsible for the broadband noise generated by the trailing edge over a wide frequency range. The broadband noise observed in Figure 2 can be observed at frequencies higher than the tonal noise.

This project consisted of two categories of experiments. The first experiment used a closed test section wind tunnel and a PIV system to obtain flow field measurements. These data provided a spatially resolved description of the turbulent velocity and vorticity field in the near wake. The second experiment was preformed in an Anechoic Wind Tunnel (AWT). This facility consists of a wind tunnel with an open test section surrounded by an anechoic room. Two free shear layers were located on the suction and pressure sides of the model to allow for the propagation of acoustic waves to the far field. More details about the AWT facility can be found in Olson and Mueller (2004). Experiments performed in this tunnel utilized unsteady surface pressure data measured simultaneously with the acoustic pressure as determined by a pair of phased microphone arrays.

PARTICLE IMAGE VELOCIMETRY

Planar two component PIV data were obtained in the plane perpendicular to the spanwise direction. Two side by side imaging areas were used in this experiment to provide appropriate spacial resolution while capturing the entire near wake region. A vector resolution of 1.5mm was achieved over an area of 110 mm by 270mm.

Instantaneous PIV Realization

A single realization of the spanwise component of vorticity with superimposed streamlines is shown in Figure 1. The trailing edge shape is outlined on the left of the figure, and the flow is from left to right. A shadow region, where data are unavailable, is located just below the trailing edge. The magnitude of vorticity has been normalized using the free stream velocity and the wake thickness parameter y_f.

The separated flow over the 45° surface contains a region of recirculation. The boundary layer vorticity separating from the model surface creates a von Karman vortex street common to wake flows. The unsteady lift that results from this wake instability is responsible for the tonal noise generated by the trailing edge.

The asymmetry of the trailing edge shape leads to a distinct asymmetry in the convected vorticity field. Specifically, the positive vorticity, originating from the lower boundary layer, is observed to form compact regions of high circulation near the trailing edge tip, which then convect downstream. In contrast, the negative vorticity, which originates from the upper boundary layer, does not exhibit this behavior. Rather, the regions of negative vorticity appears to be distributed between the regions of positive vorticity and are composed of groupings of smaller scale vortical motions.

These observations noted from Figure 1 and similar observations made from other realizations have led to a number of hypotheses about the nature of the trailing edge sound production. Specifically, the character of the small scale turbulent motions in the vicinity of the edge appears to be dependent on the "phase" location of the large scale instability. This suggests that the broadband sound produced by the smaller scale motions is modulated at the vortex shedding frequency. In the following section, the PIV results will be phase averaged to the vortex shedding phase in order to highlight the features of the turbulent flow that are responsible for tonal vs. broadband sound.

Phase Averaged PIV

The velocity field can be separated into a phase mean and a fluctuation about that value. This decomposition can be formally written in terms of the vortex shedding phase ϕ as:

$$u_i(t) = \overline{U_i(\phi)} + u_i'(\phi, t) . \tag{3}$$

This is similar to a Reynolds decomposition except that the mean is a function of the vortex shedding phase, and the fluctuations are taken about that mean rather than a stationary time average. The implication of this decomposition is that the phase mean represents the turbulent motions associated with the vortex shedding instability while all other turbulent scales averaged out. The remaining small scale turbulent structures, i.e those responsible for the creation of broadband noise, are included in the phase fluctuating component of velocity, $u_i'(\phi,t)$. The consequence of this decomposition is that it allows for the separation the turbulent motions responsible for noise generated in the tonal and broadband frequency regimes. This interpretation of equation (3) is justified given the linearity of the inhomogeneous wave equation (1).

The application the phase averaging the trailing edge flow field described in (3) necessitates the determination of ϕ for each PIV image. This was accomplished by developing a method using the a Karhunen-Loeve (KL) decomposition of the velocity field into its respective eigenmodes. The present application of this decomposition is distinct from Proper Orthogonal Decomposition (POD) (Holmes, *et al*, 1996), although the principal is essentially the same. The eigenmodes for this decomposition have been shown to be related to fluid structures in the flow and the eigenvalues to the average energy content of those structures. The motivation for the KL decomposition was to investigate which eigenmode represented the large vortical structures observed in the instantaneous PIV data. It was discovered that the first fluctuating eigenmode was related to the vorticity inherent to the wake instability and that the projection of this eigenmode onto each instantaneous PIV realization was able to provide the phase of that realization. The $\phi = 0$ condition is chosen at an arbitrary location in the shedding process. More details about the specific process used to phase average the velocity field can be found in Shannon and Morris (2004).

Figure 3 shows an illustration of the phase averaged vorticity field as a function of the vortex shedding phase. As the phase progresses the positive vorticity from the lower boundary layer separates suddenly from the model surface, "rolls up" into the low momentum region behind the trailing edge, and convects downstream. These large scale structures remain coherent as they are accelerated downstream. The phase average of the negative vorticity originating from the upper boundary layer forms larger regions of more diffuse vorticity. The compact regions of positive vorticity appear to "impinge" on the negative vorticity as it is shed more gradually into the upper shear layer. This causes the negative (phase averaged) vorticity to be spread relatively uniformly between the compact regions of positive vorticity.

The phase averaged turbulent kinetic energy is defined as

$$k(\phi) = \overline{u_1'(\phi,t)^2} + \overline{u_2'(\phi,t)^2}, \quad (4)$$

where the subscripts *1* and *2* represent the phase fluctuating parts of the streamwise and normal components of the velocity field, respectively. This quantity can be interpreted to be the total "energy" contained in the turbulent motions not associated with the vortex shedding. The implication being that $k(\phi)$ is a measure of the relative strength of the motions responsible for the production of broadband noise. Figure 4 shows the phase averaged turbulent kinetic energy as a function of phase. Although the turbulent motions represented by $k(\phi)$ are distinct from the vortex shedding motions, it is clear from the contours in Figure 4 that the small scale fluctuations are a function of the shedding phase. Specifically, the magnitude of $k(\phi)$ varies by a factor of 2 or more in the vicinity of the sharp edge. By viewing Figures 3 and 4 simultaneously it can be observed that the largest values of $k(\phi)$ are associated with the roll up of the lower boundary layer.

It is of interest to note that the small scale turbulent fluctuations in the immediate vicinity of the sharp edge, for all phase values, appears to originate primarily from the lower boundary layer. One could hypothesize that most of the turbulence responsible for broadband acoustic scattering originates from the lower boundary layer as well. This would imply that there may be a stronger correlation between the small scale turbulence inherent to the lower boundary layer and the radiated broadband sound than would be seen for the upper boundary layer turbulence.

The observations made from the phase averaged mean and kinetic energy further support the notion that the surface pressures and far field acoustics will have a broadband signature that is modulated at the vortex shedding frequency. These ideas will be further supported in the following section through direct measurements of the surface pressure and the radiated sound field.

SURFACE AND ACOUSTIC PRESSURE MEASUREMENTS

Data acquired in the AWT included simultaneous far field acoustic pressure and unsteady surface pressure. Sound pressure levels were acquired utilizing a phased array consisting of 40 microphones. The array center was positioned a distance of 1.08m from the center span of the sharp trailing edge. General information about phased microphone array design and processing techniques can be found in Underbrink (1995) and Dougherty (2002). Information relevant to the specific arrays used in this project can be found in Olson and Mueller (2003). The unsteady surface pressure was measured utilizing two condenser microphones that were flush mounted to the upper and lower surfaces of the model 12.5mm upstream of the trailing edge. This location was chosen because most of the acoustic scattering occurs at the sharp edge.

It is of interest to examine the tonal and broadband frequency ranges of the surface pressure and acoustic signals independantlely. The tonal part of a signal can be separated by notch filtering the data at the frequency related to the shedding instability. Alternatively, broadband part of the signal can be investigated by high pass filtering above the vortex shedding frequency. This retains only the frequencies that are related to the smaller scale turbulent motions.

Of particular interest are the broadband pressure fluctuations (surface and acoustic) as a function of the vortex shedding phase. The PIV results imply that the small scale turbulence is modulated by the wake instability. Therefore, the broadband surface pressure and radiated sound pressure, created by this small scale turbulence, would also be expected exhibit this dependence on vortex shedding phase. Phase averaging the high pass filtered pressure signal required a time series of the vortex shedding phase for the data acquired. This was accomplished by notch filtering the tonal part of an unsteady surface pressure sensor located in the separated region of the trailing edge. The results was a nearly sinusoidal signal whose phase was easily determined. The pressure fluctuation statistics as a function of the phase were computed by determining the root mean square value of the broadband component of pressure $P_{rms}(\phi)$ phase locked to this signal.

Phase Averaged Surface Pressure

Figures 6 shows the modulation of the root mean square pressure in the broadband frequency range with shedding phase. The data are plotted on a decibel scale referenced to the total high pass filtered root mean square pressure fluctuations $\overline{P_{rms}(\phi)}$. Two vortex shedding cycles are displayed to show the periodicity of the data. Both surface pressure sensors show an oscillation with the shedding phase. These data demonstrate that the magnitude of the surface pressure fluctuations are modulated by the vortex shedding process. The modulations observed for the suction side sensor are observed to be larger that those on the pressure side. The higher momentum fluid attached over the pressure side sensor may not be as easily distorted by the vortex shedding motions as the fluid in the stagnant separated region.

Phase Averaged Acoustic Pressure

The phase modulation of the broadband noise measured by the phased microphone array is illustrated in Figure 7. It can be seen that the oscillations about the phase mean are not symmetric, as is the case for the surface pressure. Rather, the oscillations remain below the phase mean for most of the shedding cycle and then "spike" well above this threshold for approximately 3/8 of the cycle. The hypothesis of modulated broadband noise due to the large scale vortex shedding is supported by these results.

CONCLUSIONS AND DISCUSSION

Spatially resolved velocity data collected in the near wake of a trailing edge has revealed the presence of a von Karmen wake instability. Phase averaging these data with respect to the vortex shedding has allowed for the separation the turbulent motions responsible for noise generated in the tonal and broadband frequency ranges. It was observed from the instantaneous and phase averaged velocity data that the character of the small scale turbulence in the vicinity of the sharp trailing edge was dependant on the phase of the vortex shedding motions. The implications of this being that both unsteady surface pressure and far field acoustic pressure in the broadband frequency range would also be expected to be a function of vortex shedding phase. Modulations of the magnitude of the surface and far field acoustic pressure fluctuations with vortex shedding phase were observed for measurements taken in an anechoic wind tunnel.

The implication of the phase modulation of smaller turbulent scales by the vortex shedding is that the turbulent length scales relevant to the propagation of acoustic pressure waves will also be a function of the phase. This may be an influential factor to account for when modeling the acoustic generated by a trailing edge flows with vortex shedding. The behavior of the far field acoustics about a phase reference could be an important feature in the acoustic modeling of trailing edge noise.

ACKNOWLEDGMENTS

This research was made possible through funding from the US Office of Naval Research under Grant No. N00014-03-1-0105. Technical monitor was Ron Joslin. Technical consultation of William K. Blake is gratefully acknowledged.

REFERENCES

Blake, W. K., 1986, "Mechanics of Flow-Induced Sound and Vibration", Volume II, *Academic Press, Inc.*

Dougherty, R., Mueller, T. J. (ed.), "Beamforming in Acoustic Testing," in *Aeroacoustics Measurements*, Springer-Verlag, Berlin: 2002, pp. 62-97.

Gershfeld, J. L., Blake, W. K., Knisely, C. W., 1988, "Trailing edge flows and aerodynamic sound", *AIAA Thermophysics, Plasmadynamics and Lasers Converence*, San Antonio, TX, 88-3826-CP, pp. 2133-2140.

Holmes, P., Lumley, J. L., Berkooz, G., 1996, "Turbulence, coherent structures, dynamical systems and symmetry", *Cambridge Monographs on Mechanics*, Cambridge University Press.

Howe, M. S., 1975,"Contributionos of the theory of aerodynamic sound, with application to excess jet noise and the theory of the flute." *Journal of Fluid Mechanics*, Vol. 71, pp. 625-673.

Olson, S. and Mueller, T. J., 2004, "Phases Array Acoustic Imaging of an Airfoil Trailing Edge Flow", *11th International Symposium on Flow Visualization*, Notre Dame, IN.

Shannon, D. W., and Morris, S. C., 2004, "Visualization of Blunt Trailing Edge Turbulence", *11th International Symposium on Flow Visualization*, Notre Dame, IN.

Underbrink, J. R., 1995, "Practical Considerations in Focused Array Design for Passive Broad-Band Source Mapping Applications," Masers Dissertation, Acoustics Dept., Pennsylvania State University, Philadelphia, PA.

FIGURES

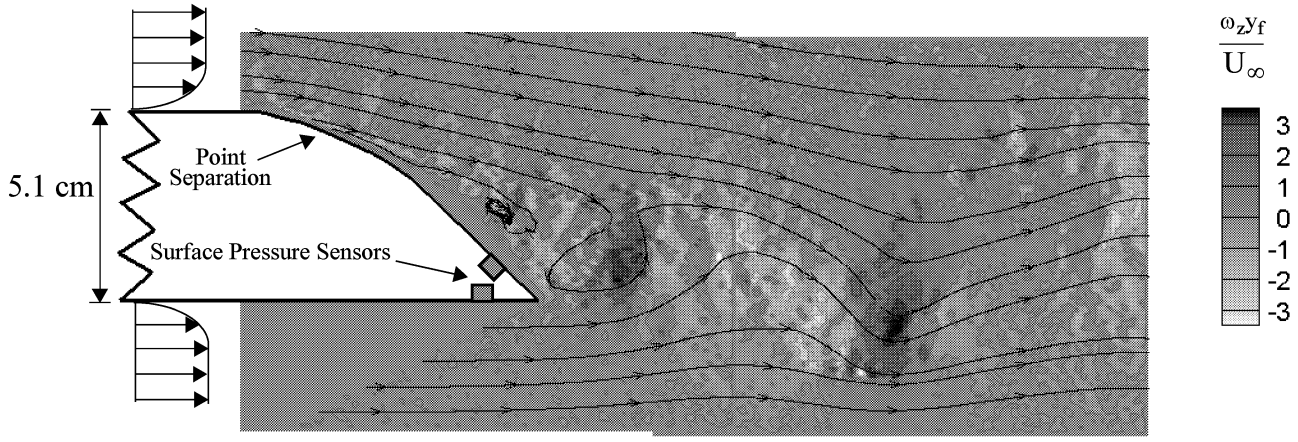

Figure 1 - Instantaneous vorticity field with streamlines. Flow is from left to right. The model has a thickness to chord ratio of 1/18 and an asymmetric 45° beveled trailing edge. Surface pressure sensors are located 12.5 mm upstream of the sharp edge.

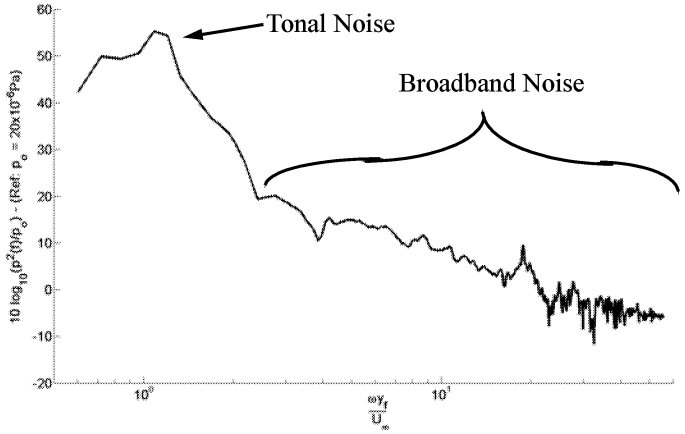

Figure 2 - Sound pressure level spectra as measured by phased arrays.

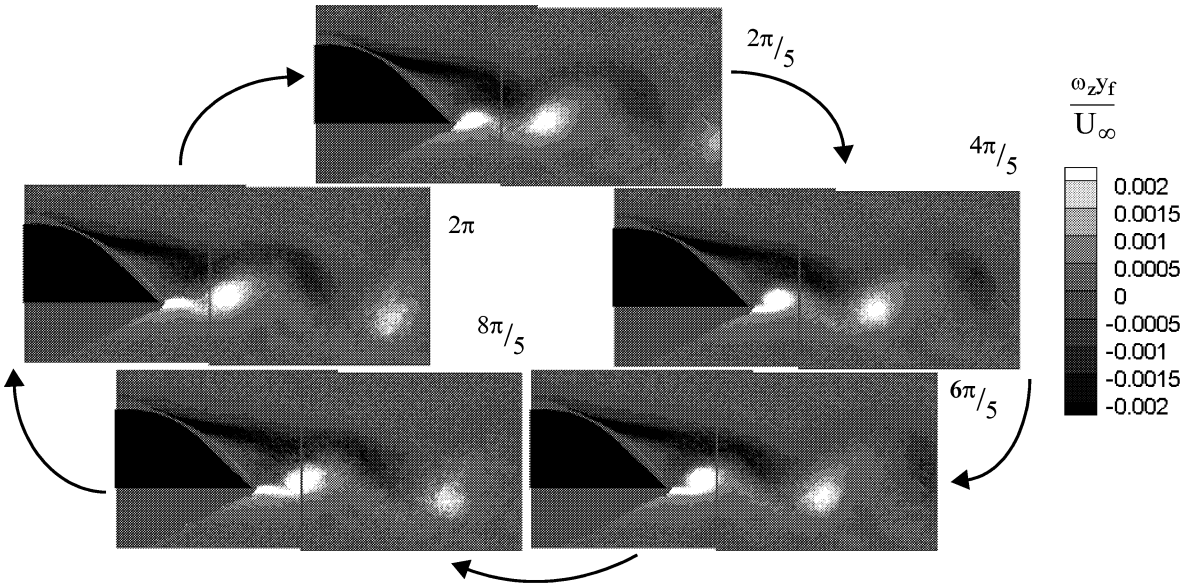

Figure 3 - Contours of vorticity as a function of vortex shedding phase.

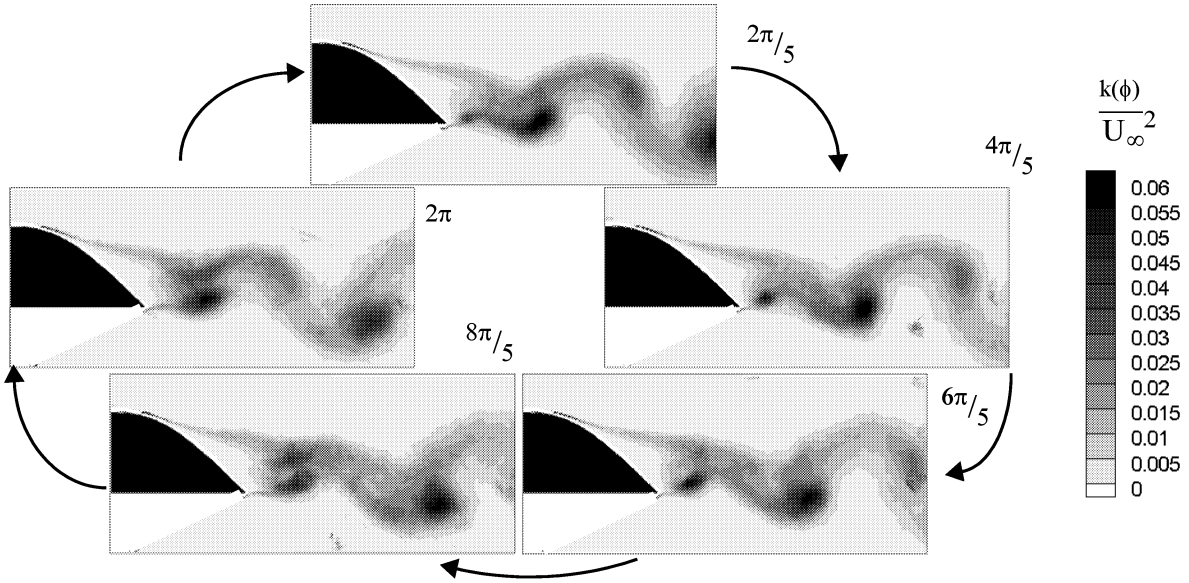

Figure 4 - Contours of turbulent kinetic energy as a function of vortex shedding phase.

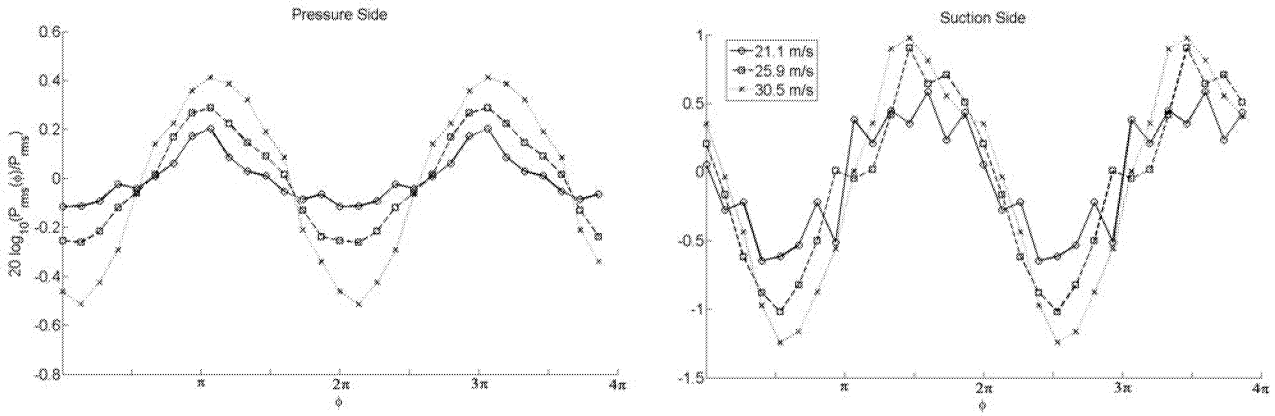

Figure 5 - Phase fluctuating part of broadband unsteady surface pressure signal.
Referenced to the broadband root mean square pressure.

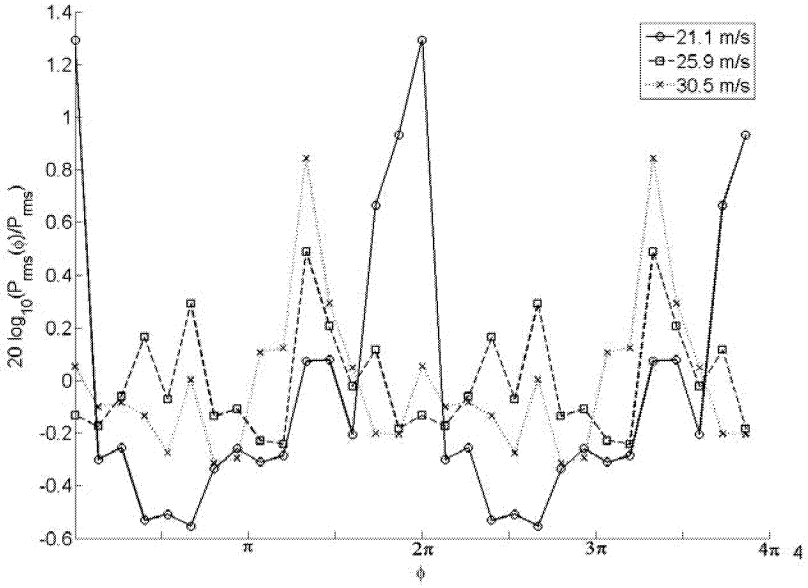

Figure 6 - Broadband sound as a function of vortex shedding phase.
Referenced to the broadband root mean square pressure.